

Wetting Behavior of Thermally Bonded Polyester Nonwoven Fabrics: The Importance of Porosity

Lu Zhu,¹ Anne Perwuelz,² Maryline Lewandowski,² Christine Campagne²

¹College of Textiles, Donghua University, Shanghai, 200051, People's Republic of China

²Laboratoire de Génie et Matériaux textiles, UPRES EA2461, Ecole Nationale Supérieure des Arts et Industries Textiles, Roubaix, France

Received 18 November 2005; accepted 19 December 2005

DOI 10.1002/app.24008

Published online in Wiley InterScience (www.interscience.wiley.com).

ABSTRACT: The wetting properties of thermally bonded polyester nonwoven fabrics with different basis weights were studied. These nonwovens had the same composition: 85% poly(ethylene terephthalate) and 15% poly(butylene terephthalate) fibers. Two techniques, the 3S wicking test and sessile drop method, yielded similar water contact angles for all the nonwovens, but these results differed from the values obtained with the single fibers. In the nonwoven fabrics, the pore structure played a dominant role in the wetting properties: the existence of large pores in the thinner nonwovens reduced the dimensions of the liquid–solid interfacial perimeter. Compared with the water contact angle

of the constituent single fibers, the contact angle of the fabrics was increased. A crenellated surface model was created to quantify the influence of pores on the wettability of nonwovens. It was possible to deduce the surface porosity of the fabric with this model, but only in the case of contact with nonwetting liquids such as water: this surface porosity corresponded only to the outermost layers of the fabric structure. © 2006 Wiley Periodicals, Inc. *J Appl Polym Sci* 102: 387–394, 2006

Key words: fibers; nonwoven fabrics; surfaces

INTRODUCTION

The interaction between liquid and fibrous assemblies plays an important role in the textile industry, including the processes of manufacturing, dyeing, and finishing. In this article, the wetting behavior of nonwoven fabrics is studied. Nonwovens are technical textiles that are manufactured from a sheet or web of directionally or randomly oriented fibers bonded by friction, cohesion, or adhesion. The fibers may be of natural or man-made origin, in staple or continuous filament form, or can be formed *in situ*. Nonwoven fabrics find applications in many fields such as hygiene products, industrial wipes, surgical packs, and filter materials.

Liquid wetting on the surface of fibrous assemblies is a topic of fundamental interest. In this process, the solid–vapor interface is displaced by the solid–liquid interface. The surface tension in the equilibrium of the three-phase boundary is given by Young's equation:

$$\gamma_{SV} - \gamma_{SL} = \gamma_{LV} \cos \theta_Y \quad (1)$$

Correspondence to: M. Lewandowski (maryline.lewandowski@ensait.fr).

Contract grant sponsor: Asia-Link Programme (initiated by the European Commission).

Journal of Applied Polymer Science, Vol. 102, 387–394 (2006)
© 2006 Wiley Periodicals, Inc.

where γ_{SV} , γ_{SL} , and γ_{LV} are the solid–vapor, solid–liquid, and liquid–vapor interfacial tensions, respectively, and θ_Y is the equilibrium contact angle.¹ For low-energy surfaces such as polymers, the surface free energy in the presence of vapor (γ_{SV}) can be assumed to be very close to the intrinsic value (γ_S).

The contact angle is an important characteristic parameter used to describe the wetting processes. A contact angle of less than 90° means good wetting between the liquid and solid, and capillary action will take place, whereas a contact angle of 90° or more indicates poor wetting, and this means that the liquid will not flow by capillarity.

Three methods are commonly used in contact-angle measurements. The first two methods are direct measurement techniques: the sessile drop method and the captive bubble method.² In the sessile drop method, a static contact angle is usually measured, and the solid surface is assumed to be smooth. The captive bubble method can be used only under conditions in which the density of the captive air bubble or liquid drop is lower than that of the liquid in which the solid is immersed. The contact angle measured by these methods is often influenced by factors such as the drop size or the surface characteristics of the solid.^{3–8}

The third method is the Wilhelmy plate technique. The wetting force at the liquid–solid interface (F_w) is measured by an electrobalance when a solid comes into contact with a liquid (Fig. 1). Knowing the liquid

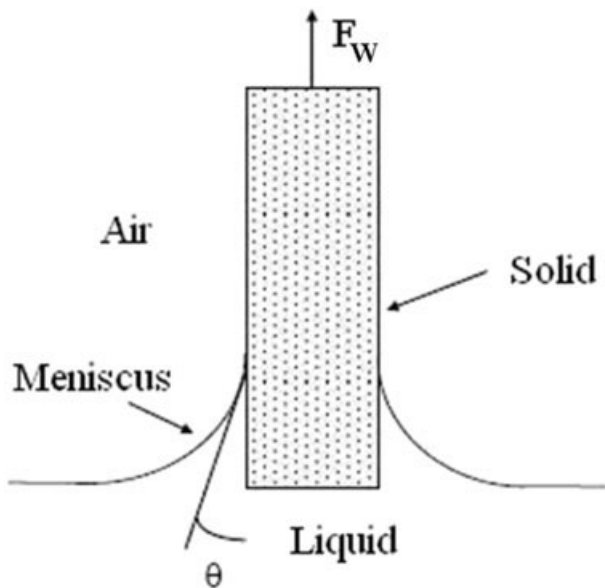


Figure 1 Schematic illustration of the experimental setup for the Wilhelmy method.

surface tension (γ) and liquid–solid interfacial perimeter (p), we can obtain the contact angle (θ) according to Wilhelmy's principle:⁹

$$F_w = p\gamma\cos\theta \quad (2)$$

The Wilhelmy plate technique has been widely used in investigating the static or dynamic contact angles of fibers^{10–12} and fibrous assemblies.^{13–15} However, it is often difficult to accurately evaluate p . The most common way of determining this perimeter is via a wetting force measurement in a total wetting liquid.^{13,16–19} Because the contact angle is zero for a total wetting liquid, p is then derived from eq. (3):

$$p = F_w/\gamma \quad (3)$$

Because the real solid surface is usually rough and heterogeneous, difficulties are encountered in both the contact-angle measurement and theory. In the work of Marmer,⁷ definitions of intrinsic, apparent, and actual contact angle are presented. Different theoretical models of rough surfaces are proposed in the studies of Tamai and Aratani,⁶ Palasantzas and Hosson,²⁰ Bico and coworkers,^{21,22} and Herminghaus.²³ In the case of fibrous assemblies, it is also difficult to quantify the wetting phenomena because of the fabric's complex geometry and the simultaneous processes of wetting and liquid penetration inside the porous structure. Furthermore, although some work has been done on the wetting properties of woven fabrics,^{13,14,16,24} few articles have been published concerning the wetting of nonwoven fabrics.

In our study, a 3S balance and a Cahn balance based on Wilhelmy's principle were used to measure the wetting properties of polyester nonwoven fabrics and their constituent fibers, respectively. The wetting force and liquid capillary absorption were deduced from the total weight measured by the electrobalance. The sessile drop method was additionally employed to compare the results for water contact angles measured by the 3S balance. The influence of the fabric basis weight on the fabric wetting behavior was also explored.

EXPERIMENTAL

Materials

Five nonwovens composed of two polyesters, 85% poly(ethylene terephthalate) (PET) and 15% poly(butylene terephthalate) (PBT), were studied. They were obtained on the same processing lines with a thermal-point spun-bonded technique. The PBT fibers were used as thermofusing fibers that, upon melting, provided cohesion to the nonwoven structure. In the final product, PBT was therefore found not in the fiber form but either in the form of small film patches or droplets across the PET fiber web. The main difference between the nonwovens was their basis weight (g/m^2), which was given by the supplier. Their characteristics are listed in Table I. The fabric thickness (mm) was measured under 0.1 kPa according to EDANA standard ERT 30.5-99 for nonwoven thickness. The fabric porosity (%) is defined by the fraction of the nominal bulk volume of the material that is occupied by void space. This parameter is calculated from the fabric's characteristics, such as the thickness, basis weight, and the material density (1.39 and 1.28 g/cm^3 for PET and PBT, respectively).

For the experiments, the samples were cut into rectangular strips (30 mm \times 50 mm). The direction in the longer dimension was in the machine direction (the direction of the web course in the nonwoven manufacture process). All samples were free from impurities.

TABLE I
Characteristics of the Nonwoven Fabrics

Nonwoven	δ (g/m^2) ^a	e (mm) ^b	ε (%) ^c
a-20	20	0.182	92.0
b-30	30	0.204	89.3
c-35	35	0.208	87.7
d-65	65	0.290	83.7
e-90	90	0.453	85.5

^a Basis weight.

^b Thickness.

^c Porosity.

TABLE II
Surface Energies of the Test Materials
(Liquids and Solids)

Liquid	γ (mN/m)	γ^d (mN/m)	γ^p (mN/m)
Distilled water	72.8	21.8	51
Silicone oil	20.4	20.4	0
Decane	23.6	23.6	0
Dodecane	25.2	25.2	0
PBT	43.65	43.6	0.05
PET	45.4	43	2.4

The testing liquids were distilled water, silicone oil (viscosity = 20 mPa s), decane, and dodecane. Table II shows their surface tension (γ), which was obtained by platinum plate tensiometry, and the values of their dispersive component (γ^d) and polar component (γ^p) found in the literature.¹⁷ The surface energies of the two polyesters obtained from the literature²⁵ are also presented in Table II.

Cahn balance

The contact angles of water on randomly sampled single fibers were measured with a Cahn balance. This apparatus included an electrobalance with an accuracy of 1 μ g and recorded the wetting force at the fiber–water interface (F_w) as a function of the immersion depth. A typical curve is shown in Figure 2. Thus, the dynamic contact angle could be determined when the stage moved up and down. The stage speed used in the study was 20 μ m/s. The advancing and receding contact angles corresponding to the advancing wetting force (F_{wa}) and receding wetting force (F_{wr}), respectively, were calculated with eq. (2).

3s wicking test

The 3S balance from GBX Instruments (France) was used to measure the liquid contact angle of the nonwoven fabrics. The apparatus mainly consisted of an

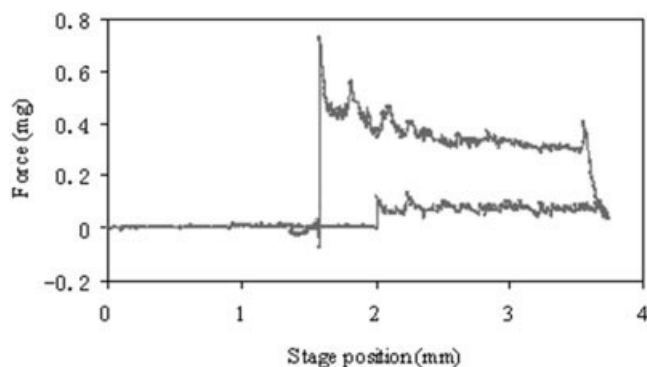


Figure 2 Wetting force as a function of the stage position for PET fiber in water.

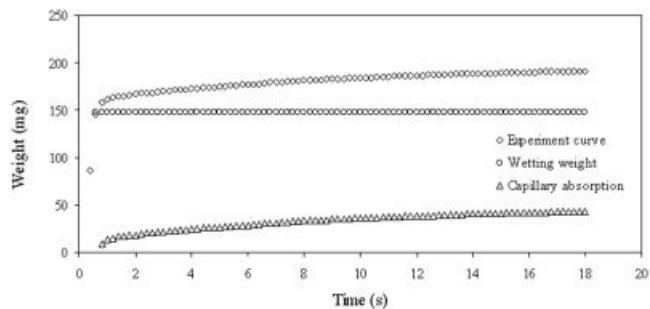


Figure 3 Experimental curve recorded by the 3S balance system and the decoupled components of the wetting weight and capillary absorption.

electronic microbalance with an accuracy of 0.1 mg, a mobile stage that could move up and down, and a data-acquisition computer station. At the beginning, the surface of the liquid reservoir was brought close to the base of a vertically suspended sample whose weight was zeroed. Then, the stage was moved up at a speed of 100 μ m/s and was stopped when a weight change of more than 2.5 mg was detected. This corresponded to the formation of a meniscus due to the wetting force (Fig. 1).¹⁷ At the same time, the liquid flowed into the fabric by capillarity, and the relationship between the total weight and time was recorded, as shown in Figure 3. When the total weight reached a constant value, the experiment was ended. The liquid absorption weight at saturation (W_{as}) was read from the screen directly when the fabric was separated from the liquid. In general, the experiment time was in the range of 120–300 s. Because the characteristic time for the meniscus rise was much less than 1 s,²⁶ the wetting force could be considered constant. Its value was obtained by the subtraction of $W_{as}g$ (where g is the acceleration due to gravity) from the total force (F_t) at the end of the experiment:

$$F_t = W_t g = F_w + W_{as} g \quad (4)$$

where W_t is the weight recorded at time t .

The contact angle was then deduced from eq. (2), perimeter p being that at the nonwoven–liquid interface. When the contact angle of water was measured, however, the wetting force was hard to detect with the apparatus. Generally, when a vertical fabric touches the surface of a liquid, a positive meniscus quickly forms around the hydrophilic fabric [Fig. 4(a)]. However, for a hydrophobic polyester nonwoven, water has poor wettability: this was evident in the preliminary observation of a drop on the nonwoven surface (Fig. 5). Therefore, when the bottom line of the polyester nonwoven just came into contact with water, a meniscus did not form spontaneously, and the wetting force could not be detected [Fig. 4(b)]. It was necessary to add a small quantity of water to the beaker to form

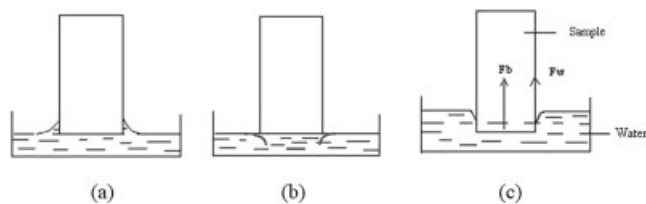


Figure 4 Illustration of water meniscus formation in different fabrics: (a) hydrophilic fabric, (b) hydrophobic fabric, (c) and hydrophobic fabric upon the addition of water.

a negative meniscus and to measure the contact angle [Fig. 4(c)]. In our experiment, after the apparatus detected the weight change and movement was stopped, water was added gradually to the beaker, 2 mL at a time, until the total weight recorded by the apparatus reached equilibrium. A typical curve of W_t versus time is shown in Figure 6.

On the basis of the Wilhelmy principle, when the water contact angle is calculated, the total force ($W_t g$) is divided into two components by a consideration of the buoyancy (F_b):

$$W_t g = F_w + F_b = p \gamma_w \cos \theta - \rho_w g V \quad (5)$$

where ρ_w is the density of water and V is the immersion volume of the sample in water. The perimeter of the water–fabric interface (p) was determined by the wetting force measurement in a total wetting liquid such as decane [eq. (3)]. The samples after 3S balance measurements in water were dried in an oven at 100°C for 5 min to evaporate the water completely. Then, the measurements with decane were performed to determine the precise interface dimension.

Sessile drop method

The contact angle between the fabric and water was additionally evaluated by the sessile drop method with a Digidrop apparatus (GBX Instruments). In this method, a water drop was deposited on the sample surface with a microsyringe, and the contact angle of

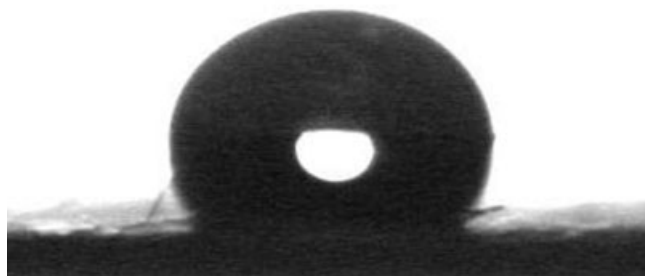


Figure 5 Water drop on the surface of a PET nonwoven fabric.

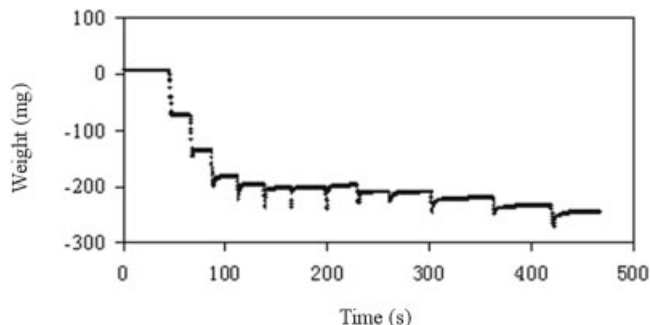


Figure 6 Typical curve of the weight versus the time upon the addition of water.

the water drop was directly measured by a video camera and calculated from the height and base diameter of the drop.

RESULTS AND DISCUSSION

Preliminary determination of the theoretical contact angles

For comparison with our results, the theoretical contact angles between PET, PBT, and the different liquids were first calculated. Indeed, in theory, if the surface free energy (γ) is assumed to depend on dispersive and polar components (γ^d and γ^p , respectively), such that $\gamma = \gamma^d + \gamma^p$, the work of adhesion (W_a) and spreading coefficient (S_e) of liquid L on solid surface S can be determined with the following equation:^{27–29}

$$W_a = 2(\gamma_{LV}^d \gamma_{SV}^d)^{1/2} + 2(\gamma_{LV}^p \gamma_{SV}^p)^{1/2} \quad (6)$$

$$S_e = W_a - 2\gamma_{LV} \quad (7)$$

If S_e is negative, the contact angle between liquid L and solid surface S can be determined by

$$W_a = (\cos \theta + 1)\gamma_{LV} \quad (8)$$

W_a and S_e were calculated for each liquid, with the surface energy values²⁵ shown in Table II. The obtained results are presented in Table III. For both solids, PET and PBT, S_e was greater than 0; that is, there was complete wetting with a zero contact angle for the three liquids: silicone oil, decane, and dodecane. With water, the contact angle values were quite high: 81.7° with PET and 96.3° with PBT.

Wetting properties of single fibers (cahn balance)

The wetting characteristics of different liquids on the surfaces of single fibers are shown in Table IV. The fiber–water interfacial dimension (p) was derived

TABLE III
Theoretical Contact Angle (θ) Values of Different Liquids on PBT and PET

Liquid	Liquid/PBT			Liquid/PET		
	W_a (mJ/m ²)	S_e (mJ/m ²)	θ (°)	W_a (mJ/m ²)	S_e (mJ/m ²)	θ (°)
Water	64.85	-80.75	96.32	83.36	-18.64	81.70
Silicone oil	59.65	18.85	0.00	59.24	59.24	0.00
Decane	64.15	16.95	0.00	63.71	63.71	0.00
Dodecane	66.29	15.89	0.00	65.84	65.84	0.00

from F_{wa} values in decane and in silicone oil with eq. (3) because the contact angle was zero with these liquids. The calculated value, 69.2 μm , was close to the perimeter dimension measured by microscopy, which was evaluated to be $66.1 \pm 3.5 \mu\text{m}$. With the mean value of the perimeter deduced from the wetting liquids, it was possible to calculate the contact angles of water with the fibers. The wetting properties of the single fibers were in accordance with the literature results for PET fibers³⁰ and with the theoretical values previously calculated (Table III). This means that all the fibers picked out from the nonwoven were composed of PET and not PBT, backing up our assumption that PBT was not in a fiber form in the nonwoven. To measure the contact angle with PBT, separate PBT fibers were obtained from an independent source. However, it was difficult to measure the water contact angle with the Cahn balance because the fibers, being very hydrophobic, showed strong repulsion with water and it was impossible to immerse them into water vertically. This confirmed the high value of the contact angle calculated theoretically (96.3°).

Wetting behavior on the surface of nonwovens: the case of wetting liquids (3S wicking test)

The contact angles of different liquids were investigated on the surfaces of nonwovens by the 3S technique. All samples had the same perimeter of 60 mm, which was measured simply by a ruler before the experiments. The results are presented in Table V: a θ value close to 0° (i.e., case of total wetting) means that $\cos \theta$ is close to 1. Silicone oil, decane, and dodecane totally wetted samples d-65 and e-90 but did not completely wet the thinner nonwovens (a-20, b-30, and

c-35). The composition of the surface was the same for all the nonwoven fabrics: polyester and pores. Both solid constituents of the nonwoven had theoretically a zero contact angle with these three liquids: the real wetted interfacial perimeter could thus be determined from eq. (3), as shown in Table VI. In comparison with the physical interfacial perimeter of 60 mm for all the samples, the wetted interfacial perimeter of the thickest nonwovens was quite close. For the thinner ones, however, the variation between these two perimeters increased. The reason that the wetted perimeter was smaller on thinner nonwovens was obvious from the microphotographs of the different samples (Fig. 7): as the basis weight increased, the fibrous density per unit of area increased accordingly, and there were fewer and fewer pores across the nonwoven structure. Therefore, in the low-density nonwovens, the real fiber-liquid interface was much smaller than the theoretical value of 60 mm because of the presence of large pores, and hence few fibers, at the wetting interface.

Wetting behavior of water on nonwovens

Two methods were used to measure the water contact angles: sessile drop and 3S measurement. Water showed poor wetting on polyester nonwovens (Table VII): the measured contact angles were all greater than 90° and ranged from 102 to 121°. There was no obvious difference among these five nonwovens, and both methods gave close values of the contact angles.

The contact angles of water on the five nonwovens were much larger than those of the constituent single fibers in our study (cf. Table IV). The high porosity of the nonwovens was one factor responsible for the

TABLE IV
Wetting Characteristics of Single PET fibers

Liquid	F_{wa} (μN)	F_{wr} (μN)	θ_a^a	θ_r^b	P (μm)
Silicone oil	1.36 ± 0.04	1.36 ± 0.05	0	0	66.4
Decane	1.72 ± 0.03	1.74 ± 0.08	0	0	72.0
Water	0.68 ± 0.09	3.04 ± 0.34	82.3 ± 1.0	52.8 ± 4.8	—

^a Advancing contact angle.

^b Receding contact angle.

TABLE V
Contact Angle (θ) Values of Different Liquids on the Surfaces of Nonwovens

Nonwoven	$\cos \theta$		
	Silicone oil	Decane	Dodecane
a-20	0.768 ± 0.071	0.805 ± 0.066	0.781 ± 0.059
b-30	0.942 ± 0.015	0.958 ± 0.004	0.959 ± 0.028
c-35	0.968 ± 0.008	0.963 ± 0.020	0.987 ± 0.024
d-65	0.98 ± 0.002	0.973 ± 0.007	1.000 ± 0.020
e-90	0.997 ± 0.010	0.998 ± 0.017	1.000 ± 0.009

increase in the contact angle. It is known that if a solid surface is ideally smooth and homogeneous, the contact angle can be predicted by Young's relation [eq. (1)]. However, if the solid surface is very rough and contains a lot of pores (Fig. 7), the contact angle will be modified.^{20–23} A liquid drop with a large equilibrium contact angle may not completely wet the solid surface. Such an incompletely wetted surface, where air is entrapped between the liquid and solid, is called a *composite interface*.⁴

In our study, the nonwoven fabrics were composed of 85% PET fibers, 15% PBT, and pores. A crenellated surface, which includes three components (solid 1, solid 2, and air), can be considered a theoretical model to quantify the effect of surface pores on the contact angles (Fig. 8).²² ϕ_1 and ϕ_2 represent the percentages of solid 1 and solid 2 in the whole solid, respectively. If the contact line has a little displacement (dx) on the composite surface, the change in the surface energy (dF) is as follows:

$$dF = (1 - \varepsilon_s)[\phi_1(\gamma_{s_1L} - \gamma_{s_1V}) + \phi_2(\gamma_{s_2L} - \gamma_{s_2V})]dx + \varepsilon_s\gamma_{LV}dx + \gamma_{LV}dx \cos \theta \quad (9)$$

where γ is the surface energy (subscripts s_1 and s_2 refer to solids 1 and 2, respectively; L and V as usual refer to liquid and vapor) and θ is the contact angle of the crenellated surface. ε_s , defined as the surface porosity, is the fraction of the surface pores in which air is entrapped. When surface energy F reaches a mini-

TABLE VI
Wetted Interfacial Perimeters of Nonwovens Deduced from the Total Wetting Liquid Experiments

Nonwoven	Wetted interfacial perimeter (mm)		
	Silicone oil	Decane	Dodecane
a-20	46.1 ± 4.3	48.6 ± 3.6	47.5 ± 3.6
b-30	56.5 ± 0.9	57.5 ± 0.3	56.5 ± 1.6
c-35	58.1 ± 0.5	57.8 ± 1.2	58.1 ± 1.4
d-65	58.8 ± 0.1	58.4 ± 0.4	59.9 ± 0.8
e-90	59.8 ± 0.6	59.9 ± 1.0	60.5 ± 0.5

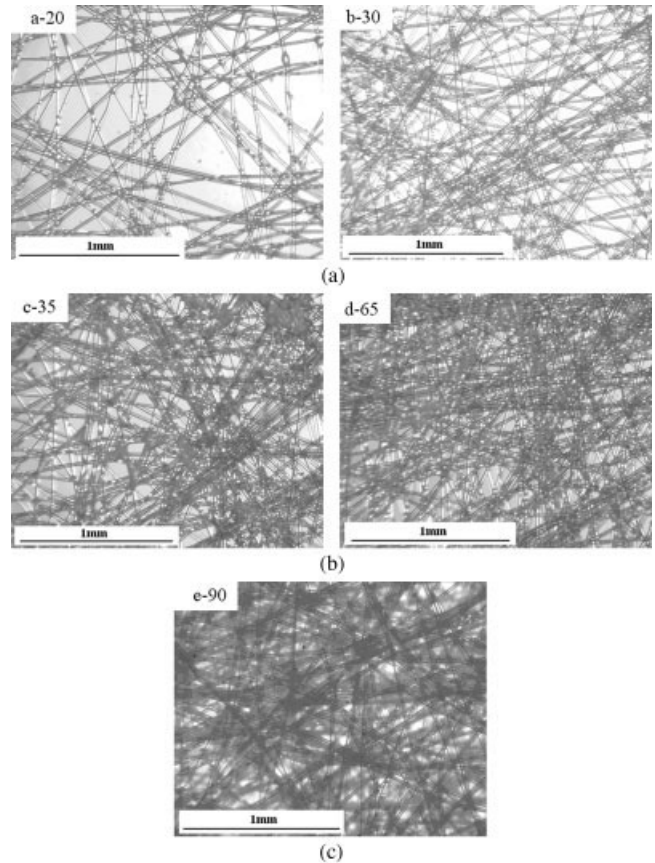


Figure 7 Microphotographs of the five nonwovens.

mum, an equilibrium contact angle can be obtained by the combination of eqs. (1) and (9):

$$\cos \theta = (1 - \varepsilon_s)(\phi_1 \cos \theta_{s_1} + \phi_2 \cos \theta_{s_2}) - \varepsilon_s \quad (10)$$

This is in accordance with the well-known Cassie–Braxter equation.³¹ If the contact angle between the PET fiber and water surface is θ_{s_1} ($\theta_{s_1} = 82.3^\circ$, as measured by a Cahn balance) and the theoretical water contact angle of the PBT solid, 96.3° , is used as θ_{s_2} , ε_s can be determined from the results of the 3S balance test with eq. (10). It is also assumed that ϕ_1 and ϕ_2 are identical on the surface as in the bulk nonwoven. The

TABLE VII
Water Contact Angles Measured by the Sessile Drop Method and 3S Balance Test

Nonwoven	Water contact angle	
	Sessile drop method	3S balance test
a-20	112.1 ± 8.0	116.8 ± 5.3
b-30	115.5 ± 6.0	119.5 ± 1.9
c-35	113.5 ± 7.6	116.4 ± 1.3
d-65	107.6 ± 5.8	112.9 ± 6.2
e-90	110.0 ± 7.4	117.8 ± 3.9

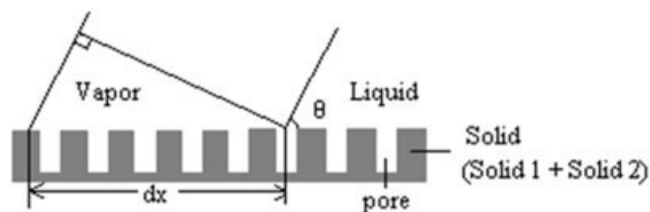


Figure 8 Crenellated surface model for the composite interface.

calculated values are tabulated in Table VIII and show that for all nonwoven fabrics, about 65% of the surface was occupied by pores that water could not wet. The surface porosity is not related to the fabric thickness or fibrous density; this can seem surprising if we consider the nonwoven images in Figure 7. This is due to the fact that water does not penetrate the structure because of the presence of hydrophobic PBT. If we consider each nonwoven as composed of a number of superposed fiber layers, the number of layers can be calculated by the division of the fabric thickness by the fiber diameter: this parameter varies roughly from 8 layers for the a-20 sample to about 20 layers for the thickest sample, e-90. The water stays in contact only with the outermost layers and does not touch the inner fibers. With a cross section of the nonwoven represented very schematically by a multiple-layer structure, the wetting behavior obtained with water and a wetting liquid is shown in Figure 9. In the case of a wetting liquid that, with both PET and PBT, presents a zero contact angle, all the pores of all the layers will be filled with liquid by capillarity. In the case of water, if the nonwoven is composed of pure PET, the contact angle being less than 90° , the liquid will penetrate the structure by capillarity. In our case, we think that PBT predominates over PET in the wetting behavior of the nonwoven: PBT in fact plays the role of a binder in the nonwoven, and even if it amounts to only 15%, it is not concentrated in small regions of the fabric but is distributed like a very thin film across the whole structure. Therefore, if we consider the case of water, the contact angle with PBT being greater than 90° , there is no wetting, and capillary action cannot occur: the nonwetting liquid cannot go past the first fiber layer, and the pores inside the structure remain empty. The

TABLE VIII
Surface Porosity Deduced from the
Cassie–Braxter Equation

Nonwoven	Surface porosity (%)
a-20	66.1 ± 5.1
b-30	68.7 ± 1.8
c-35	65.7 ± 1.3
d-65	62.3 ± 6.1
e-90	67.1 ± 3.6

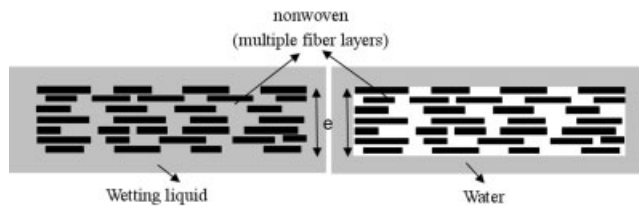


Figure 9 Top-view, schematic, cross-section representation of the wetting of a nonwoven with water or a wetting liquid.

calculated surface porosity is thus related to the porosity of this outer layer and does not take into account all the inner fiber layers and their pores, which are, however, visible on the image photographs of the nonwovens in Figure 7.

CONCLUSIONS

The contact angles of different liquids on the surfaces of polyester nonwoven fabrics and their constituent single fibers were measured with techniques based on Wilhelmy's principle. In the study of the contact between the wetting liquid and fabric, the wetting force and capillary absorption were separated from the total weight measured by an electrobalance. Because no positive meniscus could be formed when the base of the fabric came into contact with water, an improved measurement by the addition of water to the container was used. The values of the water contact angles measured by this method turned out to be close to those measured by the sessile drop method.

The wetting properties of nonwoven fabrics are influenced by their basis weight or, more exactly, by their pore structure, which is related to this characteristic. The presence of bigger pores in thinner fabrics through which a wetting liquid can go means that the real liquid–fabric interfacial perimeter that is wetted by the liquid is smaller than the measured interfacial perimeter. The water contact angle of the constituent single PET fibers measured by the Cahn balance was close to the theoretical reference, and that of PBT was calculated from the surface energies of PBT found in the literature. In comparison with the values obtained with single fibers, the water contact angle of the nonwoven fabrics was much greater. This difference was attributed to the interface, which was composed of water, polyester, and air. The surface porosity calculated by the Cassie–Braxter equation was found to be about 65% for the nonwovens of all series. This parameter was presumably related to the outermost fiber layers of the nonwoven because water could not penetrate the inner structure by capillarity.

References

1. Young, T. *Philos Trans R Soc London* 1805, 95, 65.
2. Garbassi, F.; Morra, M.; Occhiello, E. *Polymer Surface: From Physics to Technology*; Wiley: New York, 1994.

3. Drelich, J. J. *J Adhes* 1997, 63, 1.
4. Drelich, J.; Miller, J. D. *J Colloid Interface Sci* 1994, 164, 252.
5. Alberti, G.; Desimone, A. *Proc R Soc A* 2005, 461, 79.
6. Tamai, Y.; Aratani, K. *J Phys Chem* 1972, 76, 3267.
7. Marmur, A. *J Imaging Sci Technol* 2000, 44, 406.
8. Yong, C. J.; Bo, H. J.; Lee, J.; Patankar, N. A. *J Colloid Interface Sci* 2005, 281, 458.
9. Wilhelmy, L. *Ann Phys* 1863, 119, 117.
10. Sauer, B. B.; Kampert, W. G. *J Colloid Interface Sci* 1998, 199, 28.
11. Barraza, H. J.; Hwa, M. J.; Blakley, K.; O'Rear, E. A.; Grady, B. P. *Langmuir* 2001, 17, 5288.
12. Morra, M. E.; Occhiello, E.; Garbassi, F. *J Adhes Sci Technol* 1992, 6, 653.
13. Hsieh, Y. L.; Yu, B.; Hartzell, M. *Text Res J* 1992, 62, 677.
14. Hsieh, Y. L.; Yu, B.; Hartzell, M. *Text Res J* 1992, 62, 697.
15. Majid, S. A.; Young, A. K. R. A.; Young, R. A. *Ind Eng Chem Res* 1993, 32, 279.
16. Hsieh, Y. L. *Text Res J* 1995, 65, 299.
17. Pezron, I.; Bourgain, G.; Quere, D. *J Colloid Interface Sci* 1995, 173, 319.
18. Bayramli, E.; Powell, R. L. *Colloid Surf* 1991, 56, 83.
19. Wolansky, G.; Marmur, A. *Colloid Surf A* 1999, 156, 381.
20. Palasantzas, G.; Hosson, J. T. M. D. *Acta Mater* 2001, 49, 3533.
21. Bico, J.; Tordeux, C.; Quere, D. *Europhys Lett* 2001, 55, 214.
22. Bico, J.; Marzolin, C.; Quere, D. *Europhys Lett* 1999, 47, 220.
23. Herminghaus, S. *Europhys Lett* 2000, 61, 165.
24. Ibbett, R. N.; Hsieh, Y. L. *Text Res J* 2001, 71, 165.
25. Anagreh, N.; Dorn, L. *Int J Adhes Adhes* 2005, 25, 165.
26. Quere, D.; Di Meglio, J.-M. *Adv Colloid Interface Sci* 1994, 48, 141.
27. Fowkes, F. M. *J Phys Chem* 1962, 66, 382.
28. Owens, D. K.; Wendt, R. C. *J Appl Polym Sci* 1969, 13, 1741.
29. Adamson, A. W. *Physical Chemistry of Surface*, 5th ed.; Wiley: New York, 1990.
30. Vergelati, C.; Perwuelz, A.; Vovelle, L. *Polymer* 1994, 35, 262.
31. Cassie, A. B. D.; Baxter, S. *Trans Faraday Soc* 1944, 40, 549.